Kinetic Analysis of Human Flap Endonuclease-1 by Flow Cytometry†

John P. Nolan,‡,§ Binghui Shen,*,‡,|| Min S. Park,‡,⊥ and Larry A. Sklar§,▽

Life Sciences Division and National Flow Cytometry Resource, Los Alamos National Laboratory, Los Alamos, New Mexico 87545, and Cytometry, School of Medicine, University of New Mexico, Albuquerque, New Mexico 87131

Received November 30, 1995; Revised Manuscript Received June 21, 1996⊗

ABSTRACT: Human flap endonuclease-1 (FEN-1) is a structure-specific endonuclease and exonuclease which is essential for DNA replication and repair. We have cloned a human FEN-1 gene, overexpressed it in *Escherichia coli*, purified the recombinant protein to near homogeneity, and characterized its cleavage of a flap DNA structure using a novel analytical approach based on flow cytometry. With this approach, we were able to measure continuously the kinetics of DNA cleavage by FEN-1 and to separate experimentally the binding and catalysis functions of the enzyme. When the reaction was initiated by the addition of FEN-1, the cleavage kinetics were dependent on enzyme concentration and appeared to saturate at high concentrations. When enzyme and substrate were preincubated in the presence of EDTA and the reaction initiated by the addition of Mg^{2+}, rapid kinetic flow cytometry measurements showed that cleavage is fast ($t_{1/2} \sim 6$ s, $k = 0.10$ s^{-1}). Using the single-turnover kinetics as a measure of the amount of enzyme−substrate complex present, we estimated the K_d for the FEN-1−flap DNA substrate to be 7.5 nM in the absence of Mg^{2+} and the rate constant for dissociation of the enzyme-substrate complex to be 0.07 s^{-1}. Computer fitting of the experimental data to a kinetic model confirms these estimates for the individual steps and suggests some interesting features of enzymology using a surface-bound substrate.

The integrity of the human genome is maintained through the interactive processes of DNA replication, recombination, and repair. Particularly important are the fidelity of DNA replication and the specificity of DNA repair. An enzyme that contributes to these processes is the 5′−3′ exo/endonuclease flap endonuclease-1 (FEN-1). FEN-1 is essential for the maturation of Okazaki fragments. During the Okazaki fragment processing, the initiator RNA primer must be removed to complete the lagging strand synthesis in DNA replication (Konberg & Baker, 1992). In *Escherichia coli*, the 5′−3′ exonuclease activity of DNA polymerase I removes the RNA primer with the assistance of RNase HI (Funnel et al., 1986). In a reconstituted simian virus or mammalian replication system using purified calf enzymes, it was shown that the combination of 5′−3′ exonuclease and RNase HI is required for the processing of the initiator RNA (Ishimi et al., 1988; Turchi et al., 1994). Bambara's group found that calf RNase HI makes a structure-specific cleavage, removing the RNA primer as one piece, but leaving the last nucleotide at the RNA−DNA junction, which is in turn removed by a calf 5′−3′ exonuclease (Turchi et al., 1994), which is now known to be the calf homolog of FEN-1.

FEN-1 is a member of the newly emerging family of the structure-specific endonucleases. This family includes the functional homologs of FEN-1 from budding yeast (Jaquier et al., 1992; Sommers et al., 1995; Reagan et al., 1995), fission yeast (Murray et al., 1994), mouse (Harrington & Lieber, 1994a), and human (Murray et al., 1994; Hiraoka et al., 1995). This family also includes the functional homologs of xeroderma pigmentosum G (XPG), which is essential for the incision steps of nucleotide excision repair (MacInnes et al., 1993; Scherly et al., 1993, and references therein). Yeast genetic studies provide evidence that the FEN-1 homolog is involved in DNA replication, repair, and possibly recombination. The null mutants of budding yeast RTH-1 are temperature sensitive for replication and hypersensitive to methylmethanesulfonate and exhibit a hyper-recombination phenotype (Sommers et al., 1995). Most recently, the yeast RTH-1 was demonstrated to be involved in the maintenance of genomic stability. The double mutants of yeast RTH-1 and mismatch repair gene (i.e., MSH2, MLH1) have increased the incidence of microsatellite instability, suggesting that mutations in the human homolog could lead to the increased risk for types of cancer that are caused by the microsatellite instability (Johnson et al., 1995). Hereditary nonpolyposis colorectal cancer (HNPCC) has been shown to be one of these cancers.

The concept of a structure-specific nuclease was first developed by Dahlberg's group (Lyamichev et al., 1993) and further extended by others following observations of similar activities in different nucleases (Harrington & Lieber, 1994a; Murante et al., 1994; Cloud et al., 1995; Habraken et al.,

† This research has been supported by the Office of Health and Environmental Research of the Department of Energy, Los Alamos National Laboratory Directed Research Funds, and NIH Grant RR01315.

* Corresponding author. Telephone: (818)-359-8111 ext 4150. Fax: (818)-301-8972. E-mail: bshen@smtplink.coh.org.

‡ Life Sciences Division, Los Alamos National Laboratory.

§ National Flow Cytometry Resource, Los Alamos National Laboratory.

|| Current address: Department of Cell and Tumor Biology, City of Hope National Medical Center, 1500 East Duarte Rd., Duarte, CA 91010-0269.

⊥ To whom requests for reprints may also be addressed. Telephone: (505)-667-5701. Fax: (505)-665-3024. E-mail: park@telomere.lanl.gov.

▽ University of New Mexico.

⊗ Abstract published in *Advance ACS Abstracts,* August 15, 1996.

[1] Abbreviations: FEN-1, flap endonuclease-1; XPG, xeroderma pigmentosum G; HNPCC, hereditary nonpolposis colorectal cancer; FITC, fluorescein isothiocyanate; Tris, tris(hydroxymethyl)aminomethane; PBS, phosphate-buffered saline; SDS, sodium dodecyl sulfate; PAGE, polyacrylamide gel electrophoresis; IPTG, isopropyl β-D-thiogalactopyranoside; X-gal, 5-bromo-4-chloro-3-indolyl-β-D-galactoside; *Lac*I, β-galactosidase promoter repressor gene; BSA, bovine serum albumin; PEG, polyethylene glycol; EDTA, ethylenediaminetetraacetic acid; PCR, polymerase chain reaction; Km, kanamycin; MESF, mean equivalent soluble fluorescein molecules; PCNA, proliferating cell nuclear antigen.

S0006-2960(95)02840-6 CCC: $12.00

1995). Harrington and Lieber (1994a) identified an enzyme from mouse cells with a structure specificity that was originally described by Dahlberg's group with the bacterial polymerase I (Lyamichev et al., 1993). The human FEN-1 activity has been described by several laboratories and given a variety of names, including maturation factor I (MF-I, Waga et al., 1994), 5′−3′ exonuclease (Ishimi et al., 1988), and DNase IV (Robins et al., 1994). DNase IV has structural and functional homology with the 5′-nuclease domain of *E. coli* DNA polymerase (Robins et al., 1994). Several laboratories have shown that the members of the structure-specific nuclease family perform structure-specific cleavage at the junction between the 5′ unannealed tail of a primer annealed to a template. Using nuclease activity and mobility shift assays, Harrington and Lieber (1995) demonstrated that an upstream primer adjacent to the unannealed flap strand is required for efficient substrate recognition, binding, and cleavage activity. It was also found that the nuclease must enter the flap strand at the 5′ end and then slide over the entire unannealed region to the point of cleavage (Murante et al., 1995).

In order to investigate the mechanism of FEN-1 action, we cloned, expressed, and purified a recombinant FEN-1 enzyme and performed a detailed kinetic analyis using a novel flow cytometry assay. With this assay, we were able to measure FEN-1 cleavage kinetics in real time and experimentally separate its substrate binding and cleavage activities. We used these data to develop a kinetic model of FEN-1 cleavage of the DNA flap structure and fit the model to the kinetic data to confirm our estimates of the rates of individual steps. Flow cytometry is a powerful new tool for kinetic analysis of nuclease enzymes in general and provides a means to understand substrate recognition and cleavage by human FEN-1 and other structure-specific nucleases.

MATERIALS AND METHODS

Materials. Restriction enzymes, *Eco*RI, *Bam*HI, and *Nco*I, and bovine serum albumin solution were obtained from New England Biolabs (Beverly, MA). The sequenase version 2.0 DNA sequencing kit was from United States Biochemical Corp. (Cleveland, OH). Cloning vectors and XL2 blue strain were from Stratagene (La Jolla, CA). Expression vectors and the host *E. coli* strains were from Novagen (Madison, WI). All of the electrophoresis gels and reagents were obtained from Novex (San Diego, CA). Chelating Sepharose Fast Flow resin was from Pharmacia Biotech (Piscataway, NJ).

The protein quantitation assay kit was from Bio-Rad (Hercules, CA). All buffers and salts were molecular biology grade from Fisher Scientific (Pittsburgh, PA) or Sigma (St. Louis, MO). Streptavidin-coated polystyrene microspheres were from Spherotech (Libertyville, IL). FITC-labeled standard microspheres were from Flow Cytometry Standards Corp. (San Juan, PR). Sodium fluorescein was from Sigma. Oligonucleotide substrates were synthesized on an Applied Biosystems, Inc., DNA synthesizer, using biotinylated CPG resin and FITC-phosphoramidite (Glenn Research, New York). All buffers, tubes, and pipette tips were autoclaved before use, and buffer solutions used for flow cytometry were filtered through 0.2 μm pore size filters.

Molecular Cloning of the Human FEN-1 Gene. To clone human FEN-1, a pair of degenerate oligonucleotide primers were designed on the basis of consensus amino acid sequences of *Sasaccharomyces cerevisiae* YKL510 (Jacquier et al., 1992), RAD2 (Madura et al., 1986), and human XPG (MacInnes et al., 1993; Scherley et al., 1993). Polymerase chain reactions (PCRs) were performed using total plasmid DNA of a human cDNA library (kindly provided by Dr. Legerski, University of Texas M. D. Anderson Cancer Center) as a template with primers F1, 5′-AT(act)AA(ga)-CC(i)TG(tc)T(ta)(tc)GT(i)TT(tc)GA(ct)GG-3′, R1, 5′-(ga)-CA(tc)TG(i)GC(tc)TC(i)GC(tc)TCCAT(i)GG(i)GC. For amplification of FEN-1, 1 μg of library DNA was mixed with 50 pmol of each primer pair in a total reaction volume of 100 μL containing 60 mM KCl, 15 mM Tris-HCl at pH 8.8 and 25 °C, 2.75 mM $MgCl_2$, 0.5 mM dNTPs, and 2.5 units of Amplitaq DNA polymerase (Perkin-Elmer/Cetus). PCR was performed for 35 cycles of 30 s each at 94, 55, and 72 °C. PCR products were cloned into pCRscript vector according to the manufacturer's recommendations (Stratagene). The nucleotide sequence of the cloned PCR products was determined to confirm the homology with FEN-1 counterparts of the other species. Once the presence of the homology was confirmed, riboprobes were prepared using T3 RNA polymerase to screen the human cDNA library. The cDNA clones were sequenced by primer walking strategy using the modified T7 polymerase (USB).

Construction of the Overexpression Vector pET-FCH. The *Nco*I and *Bam*HI-digested DNA fragment encoding truncated FEN-1 protein was cloned into the *Nco*I and *Bam*HI site of the overexpression vector pET 28b (Novagen). In order to complete the C-terminal portion of the protein and add a purification tag of six histidines onto the C-terminus of the protein, a pair of oligonucleotides (His C1, 5′-GATCCAC-TAAGAAGAAGGCAAAGACTGGGGCAGCAG-GGAAGTTTAAAAGGGGAAAACATCATCATCA-TCATCACTA-3′; His C2, 5′-AGCTTAGTGATGATGAT-GATGATGTTTTCCCCTTTTAAACTTCCCTGC-TGCCCCAGTCTTTGCCTTCTTCCTAGTG-3′) were synthesized and cloned into the modified pET 28b vector with the N-terminus of FEN-1. The resultant clone (pET-FCH) with the intact gene and His tag was transformed into *E. coli* strain BL21(DE3).

Enzyme Expression and Purification. A single colony of pET-FCH/BL21(DE3) was picked up from the LB plate containing kanamycin (Km, 30 μg/mL), inoculated, and cultured in the liquid LB medium with Km overnight at 37 °C. The overnight saturated culture was diluted and grown at 37 °C to an OD_{600} of 0.6−0.9. Expression of the FEN-1 gene was induced by adding 0.4 mmol of IPTG. The bacterial cells were harvested after another 3 h of shaking at 300 rpm. The cell paste was frozen at −70 °C until purification.

All of the following purification steps were carried out either on ice or in a 4 °C cold room. The bacterial lysate was made by sonicating in buffer S [50 mM Tris (pH 7.9) and 100 mM sorbitol]. The extract then was centrifuged at 30000*g* for 1 h. The recombinant protein was purified by passing the supernatant over a Ni^{2+}-Chelating Sepharose Fast Flow Column (Pharmacia) under nondenaturing conditions. The column was extensively washed with buffer A [20 mM Tris-HCl (pH 7.9), 0.5 M NaCl, and 5 mM imidazole]. Buffer A containing 60 mM imidazole was used to remove weakly bound proteins. The FEN-1 protein was eluted with buffer A containing 1.0 M imidazole. The eluted protein was diluted 10-fold with PBS [50 mM sodium phosphate

(pH 7.0) and 100 mM NaCl] to prevent precipitation. The diluted protein was dialyzed with 3 L of PBS for 12 h with buffer changes every 3 h. The dialyzed protein was concentrated by applying PEG powder (molecular mass = 15−20 kDa) outside of the dialysis bag until the desired volume was obtained. The purity of the protein was assessed on a SDS−PAGE gradient gel from Novex. The protein was quantitated using a detergent-compatible protein assay (Bio-Rad). Enzyme concentrations were calculated on the basis of protein mass measurements and the predicted molecular mass of 42.5 kDa.

Assembly of the FITC−Flap Substrate and Binding to Streptavidin-Coated Microspheres. The flap DNA substrate is composed of three oligonucleotides (Figure 2): a template strand (5′-GGACTCTGCCTCAAGACGGTAGTCAACG-TGG-biotin-3′), a fluoresceinated flap strand (5′-fluorescein-GATGTCAAGCAGTCCTAACTTTGAGGCAGAGTCC-3′), and an adjacent strand (5′-CACGTTGACTACCGTC). The concentrations of oligonucleotide stock solutions were measured by absorbance at 260 nm using extinction coefficients calculated by Oligo (National Bioscience, Inc., Plymouth, MN). Fluoresceinated oligonucleotides were also measured by absorbance at 490 using an extinction coefficient of 8.0×10^4 M^{-1} cm^{-1} (Mercola et al., 1972). Fluorescein stock solutions were measured by absorbance at 490 nm using an extinction coefficient of 7.25×10^4 M^{-1} cm^{-1} (Fay et al., 1991; Nash, 1952). Cuvette fluorescence measurements were made using a SPEX 1680 spectrofluorimeter (Edison, NJ) and 1 cm square plastic cuvettes (Evergreen, Los Angeles, CA). Spectra were acquired through a 530 (±30) nm band-pass filter and were integrated, and the buffer background was subtracted using the SPEX Fluorolog software. The quantum yield of the fluoresceinated flap oligonucleotide substrate relative to fluorescein was determined to be 0.83 by comparing fluorescence measurements of the absorbance-calibrated stock solutions. The three oligonucleotides were mixed in a ratio of 1:1.5:1.5 (template−flap−adjacent) and annealed by heating the mixture to 70 °C for 5 min and allowing it to cool. Streptavidin-coated microspheres (~4×10^7/mL) were washed twice and resuspended in buffer TE [50 mM Tris and 1 mM EDTA (pH 8.0)] at a concentration of 2×10^7/mL. To measure binding to the straptavidin-coated microspheres, the indicated amount of FITC−flap substrate was added and the microspheres were incubated for at least 30 min at room temperature before being diluted 100-fold into buffer TE and analyzed on the flow cytometer.

Flow Cytometry. Flow cytometric measurements of microsphere fluorescence were made on a Becton-Dickenson FACSCalibur (San Jose, CA). The sample was illuminated at 488 nm (15 mW), and forward angle light scatter (FALS), 90° light scatter (side scatter, SSC), and fluorescence [through a 530 (±30) nm band-pass filter] signals were acquired. For kinetic measurements, time was also acquired from an internal clock in the data acquisition computer. Linear amplifiers were used for all measurements. Particles were gated on forward angle and 90° light scatter, and the mean fluorescence channel numbers were recorded. Rapid kinetic flow cytometry was performed on a specialized instrument located at the National Flow Cytometry Resource (NFCR, Los Alamos National Laboratory) which has been previously described (Nolan et al., 1995).

Kinetic experiments were started by measuring substrate beads in buffer TMB [50 mM Tris, 10 mM $MgCl_2$, and 0.1 mg/mL BSA (pH 8.0)] for ~8 s to establish a baseline. The sample tube was removed from the tube holder, enzyme added at 10 s, the tube vortexed, and sample reintroduced to the instrument. The time between mixing and data acquisition was typically 10−20 s. The mean fluorescence channel number as a function of time was calculated using the IDLYK flow cytometry data analysis program (created at Los Alamos National Laboratory), and the amount of bound FITC−flap substrate present was calculated as described above. The time value for a given data point was the midpoint of the time window measured. Cytometric measurements (fluorescence channel) were calibrated in terms of mean equivalent soluble fluorescein molecules (MESF) using commercially available standardized FITC-labeled microspheres. The MESF per bead was converted to the mean number of FITC−flap substrate molecules per bead using the relative quantum yield of the FITC−flap substrate relative to free fluorescein. The total substrate concentration was calculated from the number of FITC−flap substrates per bead and the bead concentration.

Measurement of FEN-1−Flap DNA Equilibrium Binding. When substrate beads and FEN-1 are preincubated in 1 mM EDTA, a burst of product formation is observed upon addition of 10 mM $MgCl_2$. This burst represents the amount of enzyme−substrate complex present at the time of Mg^{2+} addition. To measure the equilibrium binding, flap DNA substrate-labeled microspheres were mixed with enzyme (0−500 nM) in TEB buffer [50 mM Tris, 1 mM EDTA, and 100 μg/mL BSA (pH 8.0)]. At various times after mixing, 10 mM $MgCl_2$ was added and the reaction kinetics were measured. The burst amplitude was estimated by fitting the kinetic data to the burst equation, $F = A \exp(-k_1 t) + k_2 t + C$ (Johnson, 1995), where k_1 is the single-turnover rate constant (fixed at 0.10 s^{-1}) and k_2 is the steady rate for subsequent turnovers. The burst amplitude, A, was plotted against the FEN-1 concentration (Figure 6), and these data were fit to a hyperbolic binding equation, $[ES] = [E]_o[S]_o/([E]_o + K_d)$, where [ES] is the concentration of FEN-1−flap DNA complex and $[E]_o$ and $[S]_o$ are the total concentrations of FEN-1 and the flap DNA substrate, respectively.

Measurement of Dissociation of the FEN-1−Flap DNA Complex. The burst of cleavage following addition of Mg^{2+} to the preformed enzyme−substrate complex was used to measure the dynamics of enzyme−substrate interactions. To measure enzyme−substrate dissociation, flap DNA substrate-labeled microspheres were mixed with enzyme (100 nM) in TEB buffer and allowed to bind (8 min). The bead-bound enzyme−substrate complex was mixed with 1 μM unlabeled free flap DNA substrate. At various times after mixing, 10 mM $MgCl_2$ was added and the reaction kinetics were measured. Since the unlabeled substrate is in excess over both labeled substrate and enzyme, it is expected that any enzyme to dissociate from the labeled substrate would rebind to unlabeled substrate. The burst amplitude was estimated from the kinetic data and plotted against the time of Mg^{2+} addition (Figure 7) to give the kinetics of enzyme−substrate dissociation.

Kinetic Modeling. To refine the experimental estimates of the rate constants, we fit the enzyme dependence of the reaction time course (Figure 4b) to a kinetic model of the FEN-1 mechanism described by the following differential equations

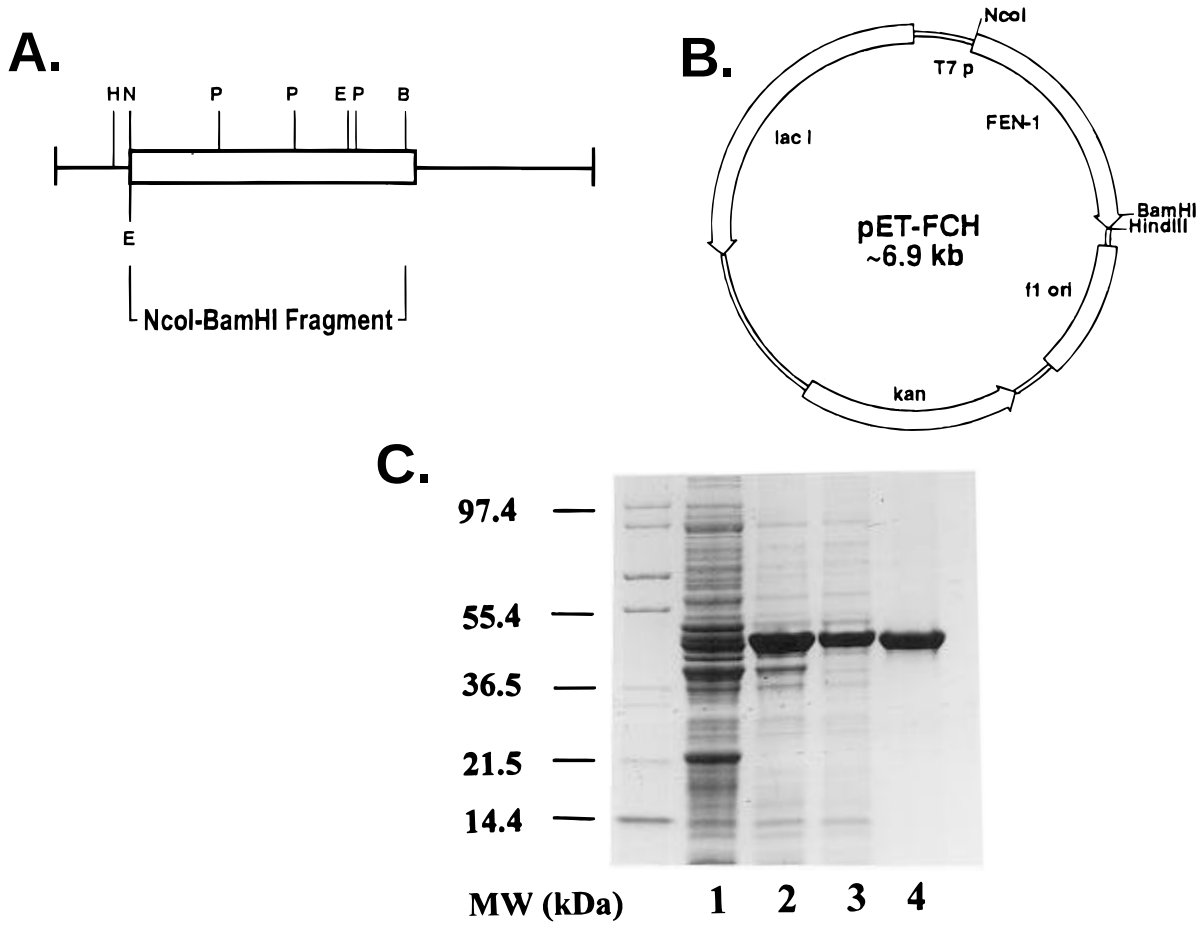

FIGURE 1: Expression and purification of FEN-1. (A) The restriction map of human FEN-1 cDNA: B, *Bam*HI; E, *Eco*RI; H, *Hin*dIII; N, *Nco*I; P, *Pst*I; S, *Sal*I; and X, *Xba*I. The box indicates the coding region of hFEN-1. (B) FEN-1 overexpression construct. The *Nco*I (containing the start codon ATG) and *Bam*HI fragment of the FEN-1 gene was subcloned into the overexpression vector pET28b with T7 RNA polymerase promoter. A pair of oligos coding for the last 17 amino acids of FEN-1, a tag of six histidines, a stop codon, and *Bam*HI and *Hin*dIII sites was cloned into the above FEN-1 expression construct, resulting in an overexpression construct with an intact FEN-1 gene and the purification tag. Plasmid map labels: T7 p, bacteriophage T7 RNA polymerase promoter; lac I, the lac repressor gene; f1 ori, phage f1 origin; and kan, kanamycin resistance gene. (C) Gel electrophoresis of total cell crude lysates, cell-free supernatant, and the purified FEN-1 on a 10 to 20% gradient SDS−PAGE: lane 1, 100 μg of untransformed *E. coli* cell lysate; lane 2, 15 μg of induced *E. coli* cell lysate with overexpression plasmid pET-FCH; lane 3, 15 μg of the soluble part of pET-FCH/BL21(DE3) crude extract; and lane 4, 5 μg of purified FEN-1 protein. The gel was stained with 0.25 g/L Coomassie Blue R-250 and destained.

$$dE/dt = -ESk_{on} + ESk_{off} + ESk_{cleave}$$

$$dS/dt = -ESk_{on} + ESk_{off}$$

$$dES/dt = ESk_{on} - ESk_{off} - ESk_{cleave}$$

$$dP/dt = ESk_{cleave}$$

and the following conservation laws

$$S_t = S + ES + P$$

$$E_t = E + ES$$

$$F = S + ES$$

where S_t and E_t are the total substrate and enzyme added, respectively, and F is the measured microsphere fluorescence. The variables k_{cleave}, k_{on}, and k_{off} represent the rate constants for substrate cleavage, enzyme−substrate binding, and enzyme−substrate dissociation, respectively, and initial values for these parameters were estimated from the experimental data in Figures 5−7, respectively. The model was fit simultaneously to the FEN-1 concentration series (Figure 4b) and optimized by simplex and least squares routines using the Scientist data fitting program (Micromath, Salt Lake City, UT). Best fits were determined by the sum of squared residuals.

RESULTS

cDNA Cloning and Purification of the E. coli-Expressed FEN-1. PCR using degenerate oligonucleotides and the total human cDNA library as a template produced two fragments: 112 and 204 bp. The 112 bp fragment was confirmed to be a part of the hFEN-1 on the basis of sequence comparison with the yeast homolog (Jacquier et al., 1992). This fragment was used as a probe to screen a human cDNA library. A clone with full length cDNA was obtained and sequenced using the primer walking strategy. The nucleotide sequence and deduced protein sequence were identical to those previously published (Murray et al., 1994; Hiraoka et al., 1995).

The *Nco*I-*Bam*HI fragment of the FEN-1 cDNA (Figure 1A) was subcloned into the pET 28b expression vector. The pair of oligonucleotides coding for the C-terminus and six histidines with *Bam*HI and *Hin*dIII sites at the ends was cloned into the pET-FEN-1 plasmid. The frame of FEN-1 expression in the resultant overexpression plasmid (pET-FCH, Figure 1B) was confirmed by DNA sequencing. When

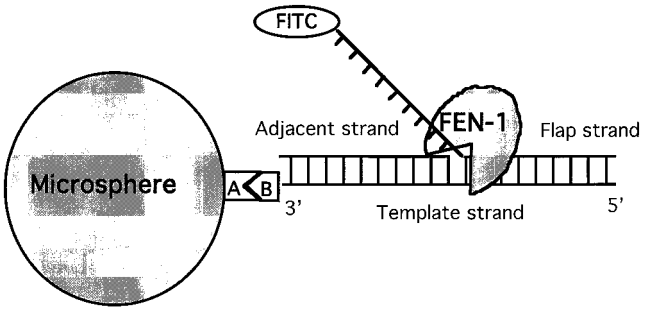

FIGURE 2: Schematic of the flap DNA−microsphere substrate: A, streptavidin; B, biotin; and FEN-1, human flap endonuclease-1.

the gene was overexpressed, about 30% of the total expressed FEN-1 protein was soluble. The FEN-1 protein was purified using a nickel-Sepharose column (Figure 1C). The yield of purified protein was approximately 1.5 mg per liter of cell culture. Both the flap endonuclease and 5′−3′ exonuclease actvities of this recombinant, histidine-tagged FEN-1 were comparable to that of calf thymus FEN-1 (also known as RTH-1), as judged by conventional assays using radiolabeled substrates (R. Bambera, personal communication).

Preparation of the FITC−Flap DNA Microspheres. The flap structure recognized by FEN-1 was assembled from three synthetic oligonucleotides: a 3′-biotinylated template strand, a 5′-fluoresceinated flap strand, and an unlabeled adjacent strand (Figure 2). The fluoresceinated flap strand and the adjacent strand were present at a 1.5-fold molar excess to ensure complete hybridization to the biotinylated strand. The annealed flap substrate was incubated with streptavidin-coated polystyrene microspheres for 30 min and the bead fluorescence measured by flow cytometry. Presented in Figure 3a−c are flow cytometric histograms of the FITC fluorescence of unlabeled beads, flap DNA substrate-labeled beads, and FITC standard beads. A binding curve revealed a linear increase in microsphere fluorescence with increasing concentrations of FITC−flap substrate up to about 90 000 molecules per microsphere (Figure 3d).

Flow Cytometric Kinetic Assay of Flap Endonuclease Activity. Flap endonuclease activity was measured by observing the decrease in microsphere fluorescence upon addition of FEN-1. The kinetics of substrate cleavage is shown as a two-parameter histogram of fluorescence vs time (Figure 4a), and total FITC−flap substrate remaining vs time (Figure 4b) is presented for a series of enzyme concentrations. The rate of cleavage increased with increasing enzyme concentrations and appeared to approach a saturating rate at the highest enzyme concentrations.

Cleavage Kinetics. The cleavage kinetics shown in Figure 4b reflect both enzyme−substrate binding and cleavage. In order to examine the kinetics of the events which follow binding, we preincubated enzyme and substrate in Mg^{2+}-free TEB buffer. After 8 min, we initiated the reaction by adding 10 mM $MgCl_2$. Under these conditions, when measured on a conventional flow cytometer, cleavage was essentially complete by the first time point after $MgCl_2$ addition (∼20 s; Figure 5, open circles). To better measure the Mg^{2+}-induced cleavage, this reaction was examined using a stopped-flow flow cytometer (Nolan et al., 1995). For these experiments, a mixture of enzyme and substrate in buffer TEB was loaded into one sample loop and a solution of buffer TEB plus 20 mM $MgCl_2$ into the other sample loop. The sample loop contents were rapidly mixed (giving a final $MgCl_2$ concentration of 10 mM). The mixed sample was

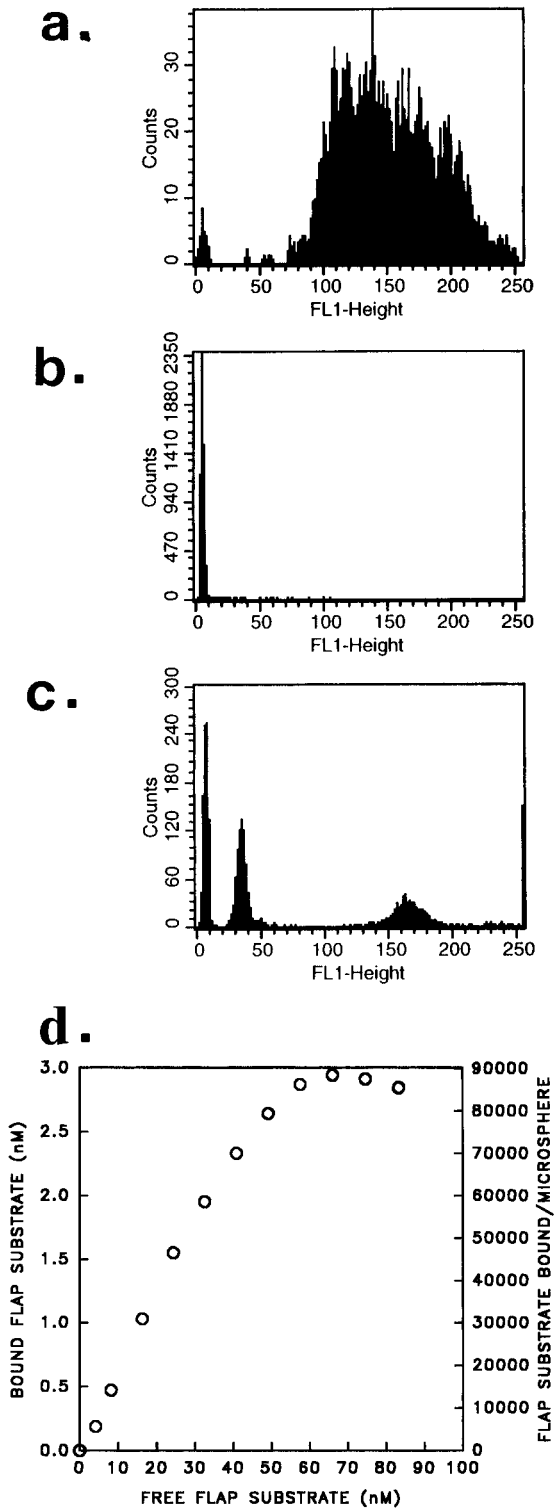

FIGURE 3: Flow cytometric histograms of FITC-labeled microspheres. Fluorescence histograms of FITC−flap-labeled microspheres (A), unlabeled microspheres (B), and FITC standard microspheres with 0, 8710, and 48 000 soluble fluorescein equivalents per bead (C). (D) Equilibrium binding of FITC−flap substrate to streptavidin-coated microspheres. Streptavidin-coated microspheres were incubated with varying concentrations of the FITC−flap substrate for 24 h and analyzed by flow cytometry.

delivered to the cytometer's point of measurement in under 1 s, and the reaction progress was measured. Rapid kinetic measurement of these kinetics revealed a half-time of approximately 7 s (Figure 5, filled circles). An exponential curve fit to these kinetics revealed single-exponential behavior and a rate constant of 0.10 s^{-1}. These data represent the single-turnover kinetics of Mg^{2+} binding, DNA cleavage,

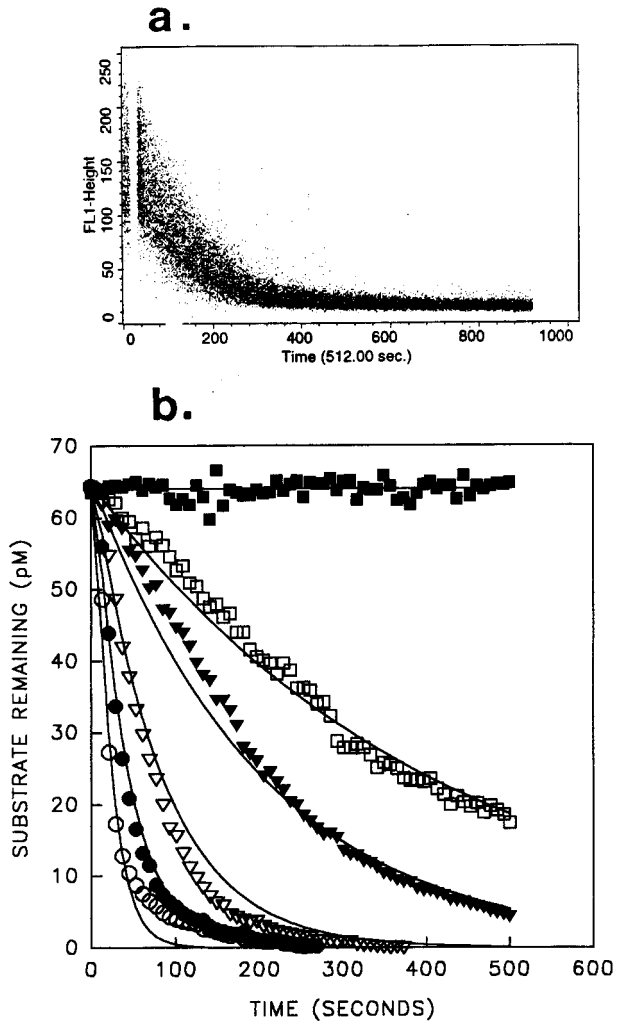

FIGURE 4: FEN-1 cleavage kinetics. (A) Two-parameter histogram of microsphere FITC fluorescence vs time. FITC−flap microspheres were measured to obtain a baseline; at 10 s, enzyme was added. (B) Flap DNA cleavage kinetics as a function of enzyme concentration. Microsphere fluorescence was acquired as in part B, and the mean fluorescence and substrate concentrations were calculated as described in Materials and Methods. Solid lines represent the best fit of the kinetic model to the experimental data. FEN-1 concentrations were 40 nM (○), 20 nM (●), 10 nM (▽), 4 nM (▼), 2 nM (□), and 0 nM (■).

and product release, independent of any enzyme binding kinetics.

FEN-1−Flap DNA Equilibrium Binding. As described above, when a saturating concentration of FEN-1 is preincubated with the flap DNA substrate in the presence of 1 mM EDTA, addition of 10 mM $MgCl_2$ induces DNA cleavage with single-exponential kinetics and a half-time of approximately 7 s (Figure 5). When the flap DNA substrate is preincubated with subsaturating concentrations of FEN-1 followed by addition of Mg^{2+}, biphasic cleavage kinetics are observed (Figure 6A): a rapid phase or burst of cleavage, corresponding to turnover of the preformed enzyme−substrate complex, followed by a slower phase, corresponding to cleavage resulting from subsequent binding and cleavage events. Thus, the burst of cleavage following addition of Mg^{2+} to enzyme and substrate which had been preincubated in the absence of Mg^{2+} is a measure of the amount of enzyme−substrate complex formed during that preincubation. We have used this approach to determine the equilibrium binding of FEN-1 to the flap DNA substrate. The amplitude of the cleavage burst (Figure 6B) increases

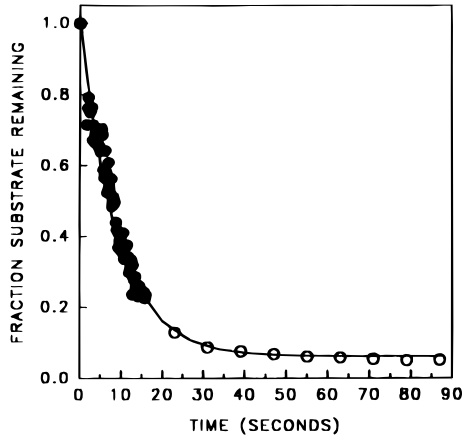

FIGURE 5: Mg^{2+}-jump kinetics. Substrate beads and saturating enzyme were preincubated for at least 5 min in buffer containing 1 mM EDTA, and then the reaction was initiated by the addition of 10 mM $MgCl_2$ and the cleavage kinetics measured using the conventional cytometer (open circles) and the Rapid Kinetic Flow Cytometer (filled circles).

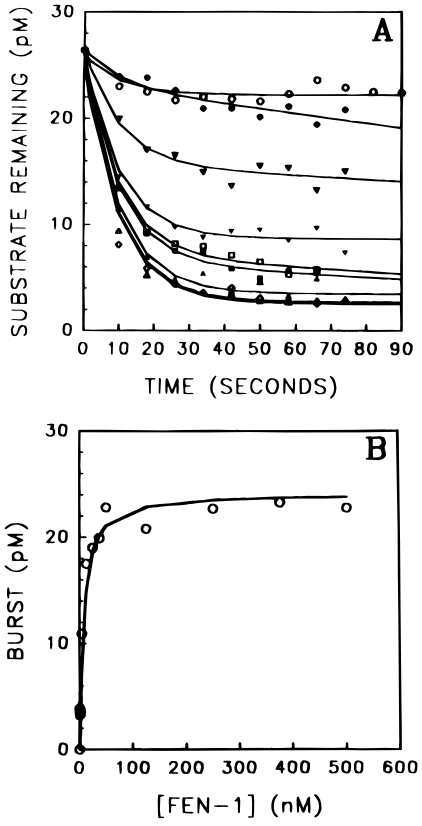

FIGURE 6: Equilibrium binding of FEN-1 and the flap DNA substrate. (A) Substrate beads were incubated in the presence of 1 mM EDTA with different concentrations of FEN-1 for 8 min. $MgCl_2$ (10 mM) was added and the cleavage kinetics recorded. FEN-1 concentrations used were 0 nM (○), 0.38 nM (●), 3.8 nM (▽), 13 nM (▼), 25 nM (□), 38 nM (■), 50 nM (△), 251 nM (▲), 502 nM (◇). (B) The burst of product formation observed in part A was plotted against the FEN-1 concentration. The solid line represents the hyperbolic fit to the data used to calculate the K_d.

with increasing FEN-1 concentrations and saturates at an enzyme concentration above several hundred nanomolar. A fit of these data to a hyperbolic binding curve reveals a K_d for FEN-1−flap DNA binding in the absence of Mg^{2+} of 7.5 nM.

Enzyme−Substrate Dissociation. Using the Mg^{2+}-induced burst of cleavage as a measure of the concentration of FEN-1−flap DNA complex present, we next investigated the

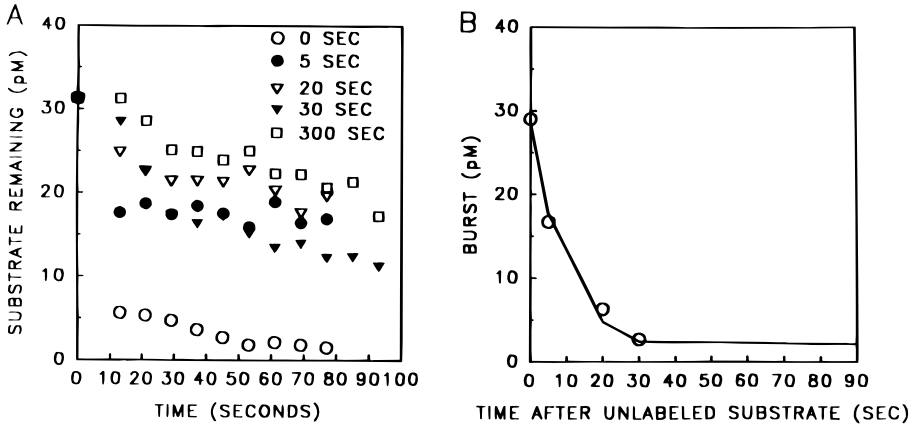

FIGURE 7: Dissociation of the FEN-1−flap DNA substrate complex. (A) Mg^{2+}-jump kinetics of samples preincubated with saturating FEN-1 for 15 min and then mixed with excess unlabeled flap substrate for different times [5 s (●), 20 s (▽), 30 s (▼), 300 s (□), and no unlabeled substrate added (○)] before addition of Mg^{2+}. (B) Amplitude of the burst of product formation observed in part A plotted against the time interval between addition of unlabeled subtrate and Mg^{2+}. The solid line represents a single-exponential fit used to calculate k_{off}.

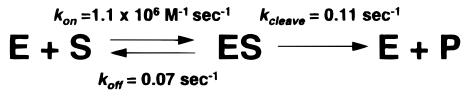

FIGURE 8: Model of the FEN-1 mechanism.

dissociation kinetics of this complex. In these experiments, we preincubated the flap DNA substrate with a saturating concentration of FEN-1 and estimated the burst of cleavage following addition of excess unlabeled flap DNA substrate. Any FEN-1 which dissociated from the labeled flap DNA substrate would not rebind to the labeled substrate but would instead bind to unlabeled substrate. The results of these experiments are shown in Figure 7. Addition of excess unlabeled substrate to the preformed enzyme−substrate complex prior to addition of Mg^{2+} results in a decreased amplitude in the cleavage burst (Figure 7A). At longer times after Mg^{2+} addition, the unlabeled flap substrate might be depleted such that cleavage of the labeled substrate is observed, but it is the rapid burst of cleavage which provides information on the concentration of the enzyme−substrate complex. The decrease in the amplitude of the burst as a function of time after addition of the unlabeled substrate is a measure of the kinetics of FEN-1−flap DNA dissociation (Figure 7B). The dissociation of the FEN-1−flap DNA complex exhibits single-exponential kinetics with a rate constant of 0.07 s^{-1} and a calculated half-time of 10 s.

Kinetic Modeling. In Figures 5 and 7, we estimated the rates of individual steps (substrate cleavage and enzyme−substrate dissociation) in the reaction sequence by varying the order of reagent addition. In order to confirm these measurements, we fit the overall reaction time course (Figure 4b) to the simplest kinetic model of the cleavage mechanism (Figure 8). Because of the heterogeneity in substrate cleavage (Figure 4), with rapid cleavage of 90% of the substrate and slower cleavage of the last 10% of the substrate, the model was fit to the first 90% of the reaction. Initial values for k_{off} and k_{cleave} came from the data in Figures 5 and 7, respectively. The data were fit (solid lines in Figure 4b) when $k_{on} \sim 1 \times 10^6$ M^{-1} s^{-1}, $k_{off} \sim 0.07$ s^{-1}, and $k_{cleave} \sim 0.11$ s^{-1}, in good agreement with the experimental estimates of the individual steps. It should be noted, however, that this model was rather insensitive to variation in k_{off} when k_{off} was less than k_{cleave} (<0.1 s^{-1}), preventing a reliable estimate of the K_d for enzyme−substrate binding in the presence of Mg^{2+}. Additionally, while the results of the kinetic modeling generally confirm the experimental measurements, the experimental data exhibit a slightly sigmoidal behavior at intermediate and low enzyme concentrations not reflected in the fit. This behavior may be unique to reactions involving surface-bound molecules, as will be discussed below.

DISCUSSION

Cloning, Expression, and Purification of Human FEN-1. In order to prepare sufficient quantities of pure FEN-1 enzyme for structure−function studies, including the detailed kinetic studies described here, we developed a bacterial expression system that produces a recombinant FEN-1 with six histidines at the C-terminus of the protein. This system allowed us to obtain several milligrams of pure and catalytically active enzyme from a 1 L culture using a simple metal chelate affinity chromatography. The histidine tag did not appear to adversely affect the enzyme activity. When the exonuclease and endonuclease activities of the recombinant human FEN-1 were compared with that purified from calf thymus, the enzyme activities were equivalent (R. Bambara, personal communication). It was previously reported that a truncated version of recombinant murine FEN-1, lacking the 17 amino acid residues at the C-terminus, exhibited endonuclease activity that was equivalent to that of the enzyme purified from mouse tissues (Harrington & Lieber, 1994). We also know that the C-terminus of XPG, which has homology with the C-terminus of FEN-1, is essential for nuclear localization but is not required for the nuclease activity of XPG (Knauf et al., 1996; Park et al., unpublished results).

Flow Cytometric System for Kinetic Analysis of Nuclease Activity. The design of a fluorescently labeled flap DNA substrate and attachment to a microsphere enables us to use flow cytometry to measure substrate cleavage. Flow cytometry provides sensitive and quantitative measurements of bead fluorescence with intrinsic resolution between free and bound label. This eliminates the need for a step to separate substrate and product and allows continuous measurement of DNA cleavage. The advantage of kinetic flow cytometry is especially evident in the single-turnover measurements initiated by a Mg^{2+} jump (Figure 5). Stopped-flow flow cytometry readily measures the initial enzyme turnover, providing a means to estimate the amount of enzyme−substrate complex present.

Kinetics of Individual Steps. By examining the kinetics of a reaction initiated by the addition of enzyme or by the addition of Mg^{2+} cofactor, we were able to experimentally separate the binding and cleavage functions of FEN-1. Preincubation of enzyme and substrate followed by the addition of Mg^{2+} resulted in cleavage which was too fast to be measured well by conventional flow cytometry. To measure the kinetics of this fast cleavage, we employed the Rapid Kinetic Flow Cytometer, an instrument capable of acquiring fluorescence signals within 300 ms of sample mixing (Nolan et al., 1995). When enzyme was present at high concentrations, Mg^{2+}-induced substrate cleavage proceeded to completion with single-exponential kinetics, representing a single turnover of FEN-1 cleavage of the flap substrate. Although the cleavage rate constants measured here compare well with reports of other nucleases (Halford & Johnson, 1983; Alves et al., 1989; Hensley et al., 1990; Zebala et al., 1992; Ghosh et al., 1994), the rate constant is smaller than would be expected if it represented the actual cleavage event. Pre-steady state kinetic analysis of DNA polymerase and reverse transcriptase mechanisms (Patel et al., 1991; Kati et al., 1992) estimates the rate constants for the exonuclease cleavage event of these enzymes at 10−100 s^{-1}, 100−1000 times faster than that measured here. This suggests that these kinetics reflect some further Mg^{2+}-dependent conformational change of enzyme−substrate complex which occurs before cleavage can take place. Such a conformational change might involve sliding of the enzyme along the DNA strand to the point of cleavage (Murante et al., 1995). Recently, it was reported that FEN-1 interacts with proliferating cell nuclear antigen (PCNA). The presence of the toroidal PCNA trimer stimulated the activity 10−50 times (Li et al., 1995), suggesting that this structure can direct FEN-1 to the cleavage site and that FEN-1 acts as part of a macromolecular complex.

At enzyme saturation, the Mg^{2+}-jump kinetics represent a single turnover of FEN-1 cleavage of the flap substrate. When enzyme is present at concentrations below saturation, the amplitude of the cleavage burst induced by Mg^{2+} addition is a measure of the amount of enzyme−substrate complex present. At subsaturating concentrations of enzyme, Mg^{2+} addition resulted in biphasic cleavage kinetics: a rapid burst of cleavage followed by a slower phase. These kinetics represent rapid turnover of the preformed enzyme−substrate complex, followed by new binding and rebinding of enzyme to substrate and subsequent cleavage cycles. The size of the rapid burst follows a hyperbolic dependence on FEN-1 concentration (Figure 6B), and indicates an equilibrium dissociation constant (K_d) of 7.5 nM for FEN-1−flap DNA complex formation in the absence of Mg^{2+}. If, after preincubation with saturating FEN-1, excess unlabeled flap substrate is added for brief intervals before Mg^{2+}, the amplitude of the rapid cleavage burst is reduced in a time-dependent manner. This decrease in the burst results from dissociation of the FEN-1−FITC−flap DNA complex and rebinding of FEN-1 to the unlabeled substrate. These dissociation kinetics have single-exponential kinetics and a rate constant of 0.07 s^{-1}.

Overall Kinetic Model. To refine these estimates, we fit the enzyme dependence of the complete reaction time course (Figure 4b) to a kinetic model of the cleavage process (Figure 8). The resulting fits (solid lines in Figure 4b) give parameter values (summarized in Figure 8) which were in general agreement with the initial experimental estimates and also reveal several interesting features of this system. First, the binding rate constant determined here is similar to that for diffusion-limited binding of a similar-sized molecule to a surface-bound ligand, that of a Fab antibody fragment binding to a liposome-bound antigen (Petrossian et al., 1984). Second, the best fits revealed a systematic error in the last 10% of the reaction kinetics, where the observed kinetics were slower than those predicted by the model. This could be due to surface inhomogeneity of the microsphere resulting in a slightly reduced accessibility of substrate to enzyme. This possibility could be tested by constructing the flap substrate from longer oligonucleotides, where the cleavage site is farther from the surface of the bead. Third, a slightly sigmoidal shape is apparent in the experimental curves. This behavior is likely a peculiarity of enzyme action on a surface-bound substrate. The enhanced rebinding of ligand to surface-bound receptor has been described (Goldstein et al., 1989; Erickson et al., 1987) and depends on the binding rates and receptor suface densities. The estimated binding constants and surface densities observed here are on the same order of magnitude as the conditions where this is predicted to occur. This possibility could be further evaluated by systematically varying the flap DNA substrate surface densities and constructing models with an additional rebinding step. Finally, the apparent K_d for enzyme−substrate binding is 7.5 nM, measured in the absence of Mg^{2+} (Figure 6). Because the fits are relatively insensitive to off rates less than the cleavage rate (<0.1 s^{-1}), the K_d (k_{off}/k_{on}) in the presence of Mg^{2+} is not well-defined. It is possible that addition of Mg^{2+} to the system induces a conformational change in the enzyme, the DNA, or both. The experimental approach of measuring binding in the absence of an essential cofactor is often used, but results need to be considered in the context of the enzyme's native environment where Mg^{2+} is always present.

Comparison of New and Existing Technology. Traditional methods for assaying enzymatic activity of restriction endonucleases have relied on gel electrophoretic analysis of cleaved DNA substrates (Perbal, 1984; Halford & Goodall, 1988). Synthetic oligonucleotides have also found application in a number of restriction enzyme kinetic studies, in which product formation has been monitored by gel electrophoresis, filter binding, homochromatography, or HPLC (McLaughlin et al., 1987; Alves et al., 1989; Fliess et al., 1986). All these methods share the limitations of discontinuous sample handling at fixed time points followed by a separation step for resolution of product and substrate. Often, radiolabeling of the substrates is required to afford the sensitivity necessary for detecting strand scission at low substrate concentrations. Spectroscopic methods for measuring nuclease activity have been reported which provide continuous kinetic resolution. Tryptophan fluorescence has been used in stopped-flow measurements of *Eco*RI endonuclease activity (Alves et al., 1989). This approach provides molecular scale information about enzyme conformation, but tryptophan fluorescence does not allow particularly sensitive measurements (800 nM substrate, 200 nM enzyme). A more general assay for nuclease activity takes advantage of fluorescence resonance energy transfer from FITC to rhodamine to discriminate product from substrate (Ghosh et al., 1994), providing somewhat better sensitivity (10 nM substrate, 50 pM enzyme).

The flow cytometric flap endonuclease activity described here has several advantages over traditional assays. First,

because flow cytometry provides intrinsic discrimination between particle-bound and free fluorophore, we are able to continuously measure the reaction kinetics of the cleavage of microsphere-bound fluorescent substrate. Real-time analysis of enzyme kinetics allows a variety of mechanistic studies to be performed. Second, the sensitivity of the fluorescence assay is enhanced by assembling the substrate on a microsphere. Though the total concentration of substrate in solution is low (50−100 pM), when a single microsphere containing 100 000 substrate molecules is measured in the flow cytometer's probe volume (20 pL), the flow cytometer measures an effective concentration of 8 nM. The ability to measure low concentrations of substrate makes it easier to provide enzyme in excess and thus to measure single-turnover kinetics. The assay will detect contaminating nucleases from nonsterile pipette tips, tubes, etc. Third, the assay is robust. Stored properly, the substrate−bead complex is stable for several weeks in the refrigerator. When this assay is used to determine a single end point, as might be used when testing column fractions during purification, samples can be analyzed at a rate of about two per minute. This combination of high sample through-put and real-time kinetic measurement should make kinetic flow cytometry a useful and general tool for the study of cleavage of biological polymers.

In summary, we have purified the human FEN-1, a member of a newly emerging family of structure-specific endonucleases involved in DNA damage and repair. Using a novel flow cytometric assay system for bead-bound substrate, we have characterized the kinetic steps of FEN-1 cleavage of a flap DNA structure. The assay and analysis established here will be very useful in future studies of the molecular mechanisms of FEN-1 action, as well as in characterizing other members of this enzyme family, especially when combined with molecular and structural biological approaches.

ACKNOWLEDGMENT

We thank Ms. Kieran G. Cloud for synthesis of all the oligos used in the experiments, Mr. Robb C. Habbersett for customizing the IDLYK flow cytometry data analysis program to facilitate kinetic analysis, Dr. Ronald Gary for the stimulating discusion and critical reading of the manuscripts, and Dr. Randy Legerski at the University of Texas M. D. Anderson Cancer Center, Houston, TX, for providing us the human cDNA library.

REFERENCES

Alves, J., Ruter, T., Geiger, R., Fliess, A., Maass, G., & Pingoud, A. (1989) *Biochemistry 28*, 2678−1284.
Cloud, K. G., Shen, B., Strniste, G. F., & Park, M. S. (1995) *Mutat. Res. 347*, 55−60.
Erickson, J. W., Goldstein, B., Holowka, D., & Baird, B. (1987) *Biophys. J. 52*, 657−662.
Fay, S. P., Posner, R. G., Swann, W. N., & Sklar, L. A. (1991) *Biochemistry 30*, 5066−5075.
Fliess, A., Wolfes, H., Rosenthal, A., Schwellnus, K., Blocker, H., Flank, R., & Pigoud, A. (1986) *Nucleic Acids Res. 14*, 3463−3474.
Funnel, B. E., Baker, T. A., & Kornberg, A. (1986) *J. Biol. Chem. 261*, 5616−5624.
Ghosh, S. S., Eis, P. S., Blumeyer, K., Fearon, K., & Miller, D. P. (1994) *Nucleic Acids Res. 22*, 3155−3159.
Goldstein, B., Posner, R. G., Torney, D. C., Erickson, J. W., Holowka, D., & Baird, B. (1989) *Biophys. J. 56*, 955−966.
Habraken, Y., Sung, P., Prakash, L., & Prakash, S. (1995) *J. Biol. Chem. 270*, 30194−30198.
Halford, S. E., & Johnson, N. P. (1983) *Biochem. J. 191*, 593−604.
Halford, S. E., & Goodall, A. (1988) *Biochemistry 27*, 1771−1777.
Harrington, J. J., & Lieber, M. R. (1994a) *EMBO J. 13*, 1235−1246.
Harrington, J. J., & Lieber, M. R. (1994b) *Genes Dev. 8*, 1344−1355.
Harrington, J. J., & Lieber, M. R. (1995) *J. Biol. Chem. 270*, 4503−4508.
Hensley, P., Nardone, G., Chirikjian, J. G., & Wastney, M. E. (1990) *J. Biol. Chem. 265*, 15300−15307.
Hiraoka, L. R., Harrington, J. J., Gerhand, D. S., Lieber, M. R., & Hsieh, C. (1995) *Genomics 25*, 220−225.
Ishimi, Y., Claude, A., Bullock, P., & Hurwitz, J. (1988) *J. Biol. Chem. 263*, 19723−19733.
Jacquier, A., Legrain, P., & Dujon, B. (1992) *Yeast 8*, 121−132.
Johnson, K. A. (1995) *Methods Enzymol. 249*, 38−61.
Johnson, R. E., Kovvali, G. K., Prakash, L., & Prakash, S. (1995) *Science 269*, 238−240.
Kati, W. M., Johnson, K. A., Jerva, L. F. & Anderson, K. S. (1992) *J. Biol. Chem. 267*, 25988−25997.
Knauf, J., Pendergrass, S. H., Marrone, B. L., Strniste, G. F., MacInnes, M. A., & Park, M. S. (1996) *Mutat. Res*. (in press).
Kornberg, A., & Baker, T. A. (1992) in *DNA Replication*, W. H. Freeman and Company, New York.
Li, X., Li, J., Harrington, J. J., Lieber, M. R., & Burgers, P. M. (1995) *J. Biol. Chem. 270*, 22109−22112.
Lyamichev, V., Brow, M. A. V., & Dahlberg, J. E. (1993) *Science 260*, 778−783.
MacInnes, M. A., Dickson, J. A., Hernendez, R. R., Learmonth, D., Lin, G. Y., Mudgett, J. S., Park, M. S., Shauer, S., Reynolds, R. J., Strniste, G. F., & Yu, J. Y. (1993) *Mol. Cell Biol. 13*, 6393−6402.
Madura, K., & Prakash, S. (1986) *J. Bacteriol. 166*, 914−923.
McLaughlin, L. W., Benseler, F., Graeser, E., Piel, N., & Scholtissek, S. (1987) *Biochemistry 26*, 7238−7245.
Mercola, D. A., Morris, J. W. S., & Arquilla, E. R. (1972) *Biochemistry 11*, 3860−3874.
Murante, R. S., Huang, L., Turchi, J. J., & Bambara, R. (1994) *J. Biol. Chem. 269*, 1191−1196.
Murante, R. S., Rust, L., & Bambara, R. A. (1995) *J. Biol. Chem. 270*, 30377−30383.
Murray, J. M., Tavassoli, M., Al-harithy, R., Sheldrick, K. S., Lehmann, A. R., Carr, A. M., & Watts, F. Z. (1994) *Mol. Cell. Biol. 14*, 4878−4888.
Nash, T. (1958) *J. Phys. Chem. 62*, 1574−1578.
Nolan, J. P., Posner, R. G., Martin, J. C., Habbersett, R. C., & Sklar, L. A. (1995) *Cytometry 21*, 223−229.
Patel, S. S., Wong, I., & Johnson, K. A. (1991) *Biochemistry 30*, 511−525.
Perbal, B. (1984) in *A Practical Guide to Molecular Cloning*, pp 28−90, Wiley, New York.
Petrossian, A., & Owicki, J. C. (1984) *Biochim. Biophys. Acta 776*, 217−227.
Reagan, M. S., Pittenger, C., Siede, W., & Friedberg, E. C. (1995) *J. Bacteriol. 177*, 364−371.
Robins, P., Pappin, D. J. C., Wood, R. D., & Lindahl, T. (1994) *J. Biol. Chem. 269*, 28535−28538.
Scherly, D., Nouspikel, T., Corlet, J., Ucla, C., Bairoch, A., & Clarkson, S. G. (1993) *Nature 363*, 182−185.
Sommers, C. H., Miller, E. J., Dujon, B., Prakash, S., & Prakash, L. (1995) *J. Biol. Chem. 370*, 4193−4196.
Turchi, J. J., Huang, L., Murante, R. S., Kim, Y., & Bambara, R. A. (1994) *Proc. Natl. Acad. Sci. U.S.A. 91*, 9803−9807.
Waga, S., Bauer, G., & Stillman, B. (1994) *J. Biol. Chem. 269*, 10923−10934.
Zebala, J. A., Choi, J., & Barany, F. (1992) *J. Biol. Chem. 267*, 8097−8105.

BI952840+